1. REFINEMENT OF MODEL DESCRIPTION OF POP FATE IN THE ENVIRONMENT

The work on the refinement of model design and parameterization for simulations of POP fate in the environment is permanently ongoing in MSC-E. This year these activities were performed in the following directions.

- Preparatory work on modifications of model description of gas-particle partitioning of POPs in the atmosphere and degradation in particular-bound form. These modifications are, in particular, focused on the description of the interaction of POPs with atmospheric aerosol including elemental carbon (EC).
- Working out model description of POP emissions to the environmental media. At present stage of the work direct emissions of PCDD/Fs to soil are considered. It was shown that taking into account these emissions allows essential refining the agreement between available PCDD/F measurements and calculation results.
- Further elaboration and testing global modelling of POPs with the help of the GLEMOS system. This year vegetation module was elaborated ond involvet to GLEMOS. The result is tested by calculations of two POPs with high ability of intercontinental transport: PCB-153 and HCB.

This Chapter is devoted to the description of the results of the above-listed activities.

1.1. Sorption and degradation of particle-bound PAHs

Gas-particle partitioning is one of the main processes determining the fate of POPs in the atmosphere. The influence of this process is conditioned by the differences in behaviour of POPs in gaseous and particle-bound forms. The processes affected by gas-particle partitioning are POP degradation in the atmosphere, deposition process and gaseous exchange with the underlying surface.

At present in the description of gas-particle partitioning only two forms of particle-bound POPs are considered. They are POPs adsorbed on aerosol surface and POPs absorbed into organic fraction of the atmospheric aerosol. Such rough description is used due to the lack of knowledge on chemical composition of atmospheric aerosol and on degradation rate constants for POPs sorbed on aerosols of different chemical nature. However, recently a number of scientific papers on degradation of POPs (especially PAHs) on particles have appeared and MSC-E initiated the work on the refinement of model description of PAH degradation process based on the new obtained data [*Shatalov et al.,* 2012].

For the improvement of model description of the degradation process of particle-bound B[a]P two atmospheric processes should be considered: sorption of B[a]P on various aerosol species and degradation of B[a]P on these species due to heterogenic reactions with atmospheric reactants (ozone, nitrate compounds, etc.). The recent results of the investigation of these two processes with the focus on elemental carbon fraction (EC) in the atmospheric aerosol are presented below.

Sorption on aerosol species. At present it is recognized by all researchers that the description of gas-particle partitioning should be performed by the combined approach taking into account sorption on various aerosol species [*Lohman and Lammel,* 2004]. For realization of this approach the information on aerosol chemical composition is required. Since this composition is rather complicated and is not completely known up to the moment, three aerosol fractions are considered in the model: elemental carbon (EC), organic carbon (OC) and the rest aerosol without further specification of this

fraction. The latter fraction can include mineral aerosols, nitrates, sulfates and so on. Typical distribution of aerosol between these three fractions in different areas within the EMEP region presented in the above cited paper is shown by plots in Fig. 1.1.

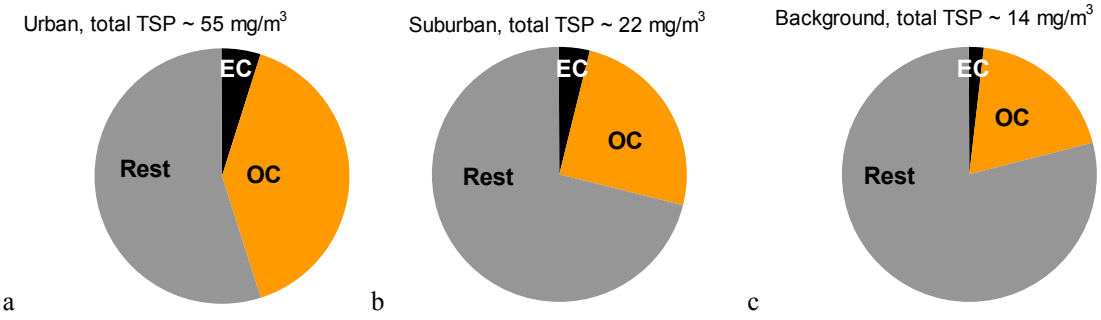

Fig. 1.1. *Distribution of the atmospheric aerosol between three considered fractions in urban (a), suburban (b) and background areas according to [Lohman and Lammel, 2004].*

For brevity, below B[a]P sorption and degradation in background areas only are considered. It is seen that the fraction of EC in the atmospheric aerosol is rather small (about 2% in the background regions). However, as will be shown below, essential part of particle-bound B[a]P is sorbed on small fraction of EC. Let us consider sorption processes in more detail.

Absorption of B[a]P into organic carbon fraction of atmospheric aerosol is described in the model by the scheme described in [*Pankow,* 1994] and [*Harner and Bidleman,* 1998]. In this papers relation between B[a]P fraction φ_{OC} absorbed in organic carbon is defined as

$$\phi_{OC} = K_p \cdot TSP/(1 + K_p \cdot TSP)\,, \tag{1.1}$$

where K_p is particle-gas partitioning coefficient given by the regression relation with oktanol-air partitioning coefficient K_{oa}

$$\log K_p = 0.79 \cdot \log K_{oa} - 10.01 \tag{1.2}$$

for PAHs. Adsorption on the surface of the rest aerosol is parameterized by Junge-Pankow scheme.

Concerning the description of B[a]P sorption on EC, it should be mentioned that there exist several approaches to the parameterization of this process. In particular, in the above sited paper the authors use the value of soot-air partitioning coefficient for B[a]P equal to $1 \cdot 10^{13}$, calculated on the basis of soot-water and air-water partitioning coefficients. This coefficient is not compared to any measurement data and has no temperature dependence. This hampers the usage of this coefficient for model parameterization.

Another approach to the calculation of partitioning coefficient $K_{EC/air}$ between air and atmospheric EC is proposed by [*Van Noort,* 2003] and then tested by the comparison between calculated values and available measurement data in [*Jun and Balasubramanian,* 2009]. This approach is based on regression relation between $K_{EC/air}$ and P_{ol}.

$$\log K_p = 0.18 \cdot \log P_{ol} + 8.94 - \log\left(998/\alpha_{soot}\right), \tag{2.3}$$

where is chosen equal to 100 according to [*Bucheli and Gustafsson,* 2000].

It should be noted that the values of $K_{EC/air}$ calculated by these two approaches can differ by about an order of magnitude. It seems that the second approach is preferable for model parameterization since it is validated against measurements and allows taking into account temperature dependence of $K_{EC/air}$. As shown in the paper, total partitioning coefficients calculated with and without EC fraction are close to each other for heavy PAH compounds (B[a]P, B[b]F, B[k]F and IP). However, for more detailed description of degradation process of particle-bound PAHs separate information on sorption on EC and inorganic aerosol is required.

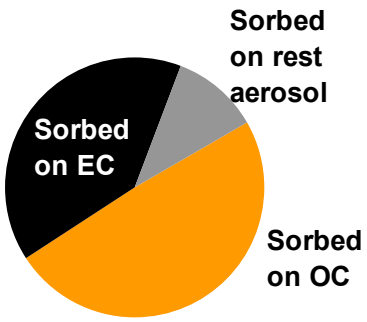

Fig. 1.2. *The distribution of atmospheric particle-bound B[a]P between elemental carbon (EC), organic carbon (OC) and inorganic aerosol (Rest) calculated on the basis of van Noort approach for background regions*

The distribution of atmospheric particle-bound B[a]P between elemental carbon (EC), organic carbon (OC) and inorganic aerosol (Rest) calculated on the basis of the above approaches is shown in Fig. 1.2. The comparison of Figs 1.1c and 1.2 shows that in spite of small EC fraction in atmospheric aerosol, noticeable part of B[a]P is sorbed on atmospheric EC. This is conditioned by the fact that B[a]P sorption on EC is about 10 times more intensive than on OC. On the opposite, the ability of B[a]P be sorbed on the rest aerosol is rather low.

Degradation process. The description of degradation process used in the current version of MSCE-POP model is based on average degradation rates for particle-bound B[a]P obtained on the basis of data from [*Chen et al.,* 2001]. However, the process of B[a]P degradation sorbed on various aerosol species was recently in the focus of investigation by a lot of researchers ([*Zhou et al.,* 2011; *Perraudin et al,* 2007; *Kwamena et al.,* 2004; *Calvert et al.,* 2002; *Pöschl et al,* 2001] and others) which allows considering the possibility of elaborating model description of degradation process taking into account sorption of B[a]P on different aerosol specied separately. In doing this, it should be taken into account that the above papers present the results of laboratory research obtained by laboratory experiments with the use of artificial media, and their results can differ by an order of magnitude and more. However, these data can be used for rough comparison of degradation half-lives for B[a]P sorbed on different aerosol species (Fig. 1.3).

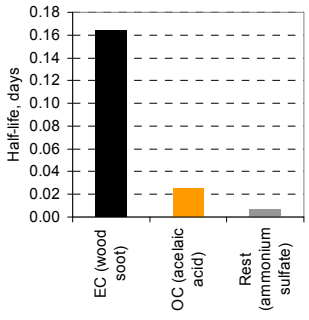

Fig. 1.3. *Half-lives due to degradation of particle-bound B[a]P. Data from [Zhou et al., 2011; Kwamena et al., 2004; Calvert et al., 2002].*

It is seen that half-lives of B[a]P sorbed on elemental carbon are essentally higher than those for B[a]P sorbed on organic carbon and inorganic aerosol. So, separate consideration of degradation of B[a]P sorbed on different aerosol fractions can essentially change model parameterization of the degradation process.

As mentioned in the previous Status Report [*Shatalov et al.,* 2012], different degradation rates obtained for reactions of B[a]P with ozone in the above mentioned papers were tested by several models. In particular, the results from [*Friedman and Selin*, 2012] obtained with the help of global 3D model GEOS-Chem show that application of the reaction rates reported in [*Pöschl et al.,* 2001] results in large underestimates of observed concentrations. The authors claim that the *Kwamena* scheme

brings observed and modeled concentrations closest together, and has little effect on the BaP which is already well simulated by the model.

As a first step in the construction of model parameterization of degradation of particle-bound PAHs in the atmosphere the comparison of total degradation rates for B[a]P sorbed on elemental carbon, organic carbon and mineral aerosol with those obtained by the current model version was performed. In this comparison wood soot, acelaic acid and ammonium sulfate were used as surrogates for EC, OC and mineral aerosol, respectively. The distribution of particle-bound B[a]P for these comparison was taken in accordance with [*Lohman and Lammel,* 2004] (see above). Degradation rates for B[a]P sorbed on these aerosol compounds were taken from [*Calvert et al*., 2002; *Kwamena et al*., 2004 and *Zhou et al*., 2011]. The data on ozone concentrations were taken from measurements at a location in Central Europe. It was found that average annual degradation rates using degradation rate constants taken from the above papers agree by order of magnitude with those obtained by the current model version (see Fig. 1.4). However, seasonal variations of degradation rate constants are essentially different. It should be noted also that for more accurate description of B[a]P degradation the influence of solar radiation activity and ambient temperature should be taken into account. In particular, the results by [*Lazatti,* 2009] show that the intensity of B[a]P degradation process depends not only on ozone concentration levels but also on solar radiation flux.

Further work on refinement of model parameterization of degradation process taking into account sorption of B[a]P on atmospheric EC and other aerosol compounds is planned to be performed in the nearest future.

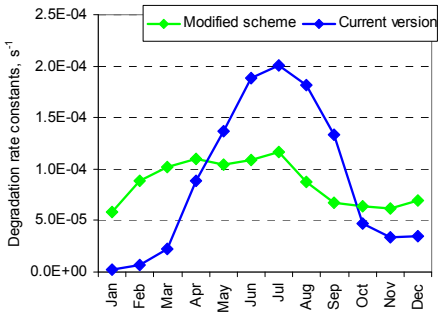

Fig. 1.4. *Comparison of degradation rate constants for B[a]P obtained by modified sceme and current calculations*

1.2. Evaluation of direct emissions to soil for PCDD/Fs

The problem of evaluation of environmental pollution by polychlorinated dibenzo(p)dioxins and dibenzofurans (PCDD/Fs) is at present of interest for a number of national and international organizations and projects (e.g. HELCOM, Swedish environmental protection agency and others). However, this task meets some differences, namely:

- Lack of regular measurements of PCDD/Fs especially in background region. In particular, no measurement data on PCDD/Fs is available under the EMEP programme.
- Gaps of the knowledge on PCDD/F properties governing the behaviour of these pollutants in the environment.
- Essential uncertainties of emission data.

Below the description of an attempt to overcome (at least, partly) the above difficulties is described.

First of all, though there are no regular measurements of PCDD/Fs in the atmosphere, a lot of measurements were performed in the course of national measurement campaigns. By literature search, MSC-E has collected over 700 individual measurements over the globe covering the period from 1990 to 2009. About 400 of these measurements are made at European locations. Main difficulty

in usage of these data is their inhomogenuity from the viewpoint of location types (from industrial to background) and measurement techniques. However, this set of data can be used for evaluation of PCDD/F pollution levels both in Europe and over the entire globe. It should be mentioned that for large part of the measurements only global toxicity is reported in literature while congener composition will be useful for model validation and evaluation of PCDD/F environmental levels. Thus, the work on collection and evaluation of PCDD/F measurements will be of high importance for investigation of environmental pollution.

Taking into account the absence of regular measurements, model assessment is the only tool for obtaining more or less complete picture of PCDD/F contamination. This study use MSCE-POP model for evaluation of PCDD/F levels in Europe. Parameterization of PCDD/F fate in the environment is made in the model according to the best available knowledge, as it was concluded by EMEP/TFMM Workshop on the review of EMEP models. Besides, model performance was earlier tested on other pollutants, such as PAHs, PCBs, HCHs and HCB and was considered in intercomparison studies.

Uncertainties of emission data can be conditioned by lack of certain emission sectors or underestimation of emissions in the available emission inventories, including emission data reported by Parties to CLRTAP to UN ECE Secretariat. The range of emission uncertainties can be evaluated from congener-specific model simulations of PCDD/F transport using official emission data only. These simulations were performed for the period from 1970 to 2010, and the resulting total toxicities were compared with available measurements. To avoid the disagreement between measurements and model results due to the use of measurement data collected at contaminated resions, such data were excluded from the consideration. The results of the comparison are shown by scatter polt in Fig. 1.5.

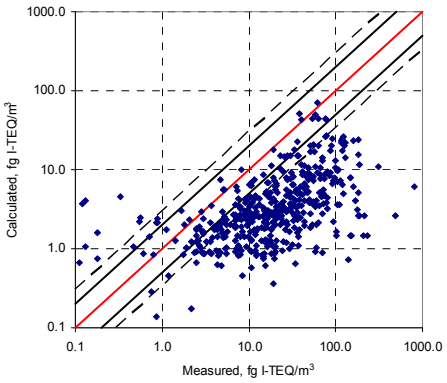

Fig. 1.5. *The comparison of PCDD/F air concentrations measured within the period from 1990 to 2010 with calculations made on the basis of official emission data.*

It was found that calculation results underestimate measured PCDD/F concentrations 5.4 times. According to the sensitivity study performed in the course of EMEP/TFMM model review, disagreement between measurements and model predictions may be about 2 times. Thus, it can be supposed that the disagreement between measurements and calculations can be conditioned (at least, partly) by underestimation of PCDD/F emissions.

At present the work on the refinement of PCDD/F emission inventories is ongoing. In particular, the UNEP Toolkit for identification of realizes of D&F was worked out in 2013.

However, there is one more reason for underestimation of PCDD/F emissions. This is the lack of direct emissions of PCDD/F to soil and water in the existing inventories. These emissions were evaluated in a number of national projects among which the EU Project “Releases of Dioxins and Furans to Land and Water in Europe” should be mentioned. This project presents sector-specific evaluation of releases of PCDD/Fs to soil and water in 17 Eropean countries in 2004. Total emissions to soil in the considered countries by sectors are shown in Fig. 1.6. Since PCDD/F emissions to water are much more uncertain, only emissions to soil will be considered below.

To evaluate to which extent taking into account emissions to soil can improve the agreement between calculations and measurements, simulations of PCDD/F transport and accumulation in the environmental media based on the official data for emissions to the atmosphere complemented by a scenario of emissions to soil were performed.

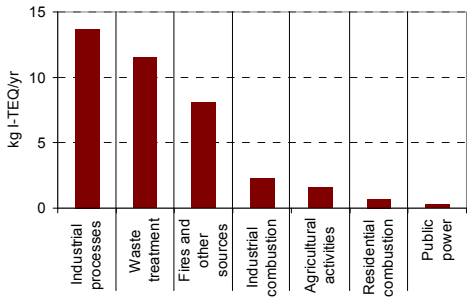

Fig. 1.6. *Sector-specific emissions to soil from 17 selected countries in 1994 according to the results of the EU Project "Releases of Dioxins and Furans to Land and Water in Europe".*

1.2.1. Elaboration of emission scenario

To elaborate the scenario of emissions to soil for calculations, emission totals in all European countries (not only in 17 countries participating in the Project) and spatial distribution of emissions for the period from 1930 to 2010 are to be estimated. The construction of the scenario is described below.

Emission totals for 1994

Evaluation of emission totals in the EMEP countries for 1994 was performed using regression between emissions from particular sectors and country characteristics namely gross domestic product (GDP), country population and area of arable lands. For each emission sector the characteristic best approximating emissions of 17 countries for the considered sector was chosen and regression coefficients were determined (see Table 1.1). Two sectors (Industrial combustion and Industrial processes) were merged into one sector since for 17 countries such merged sector showed better correlation with GDP than correlations of the two merged sectors separately.

Table 1.1. *Regression information for evaluating emission totals*

Sector	Country characteristic	Regression coefficient
Public power	GDP, mln USD	$1.83 \cdot 10^{-5}$
Residential combustion	Country population, thousands of people	$1.58 \cdot 10^{-3}$
Industrial combustion and processes	GDP, mln USD	$9.58 \cdot 10^{-4}$
Waste treatment	Country population, thousands of people	$2.81 \cdot 10^{-2}$
Agricultural activities	Arable lands area, km^2	$1.54 \cdot 10^{-3}$
Fires and other sources	GDP, mln USD	$4.84 \cdot 10^{-4}$

On the basis of the constructed regression relations emission totals for the countries not included into the EU inventory were evaluated. The results of this evaluation are shown by the plot in Fig. 1.7, where the countries included into the EU inventory are marked by green. For countries included into the EU inventory the values of emission totals given there are used.

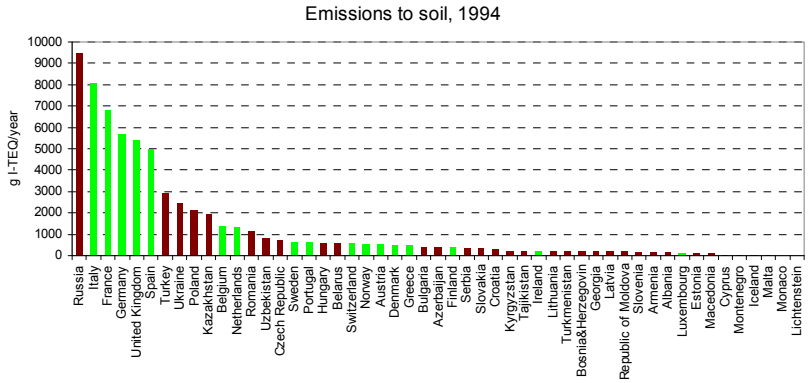

Fig. 1.7. *Emission totals in the EMEP countries in 1994 evaluated on the basis the results of the EU Project.*

Long-term trend of emissions

For evaluating PCDD/F contamination levels taking into account the accumulation of the considered pollutants in the environmental media with subsequent re-emission the values of country emissions for the whole calculation period (1930 – 2010) are needed. Since no information on emissions of PCDD/F to soil for the entire period is available, it was roughly supposed that the dynamics of emissions to soil is identical to the dynamics of emissions to the atmosphere. The latter was evaluated by official data complemented by expert estimates when needed for the period from 1990 to 2010 and by emission inventory elaborated under the POPCYCLING-BALTIC project for the period from 1970 to 1990. For the rest of the period (1930 – 1970) extrapolation of POPCYCLING-BALTIC data was used. The resulting trend of total emissions to soil for the required period is presented in Fig. 1.8. The trend is characterized by growth of emissions from the beginning of the period to 1980, strong emission reduction from 1980 to 2000 and more temperate reduction beginning from 2000.

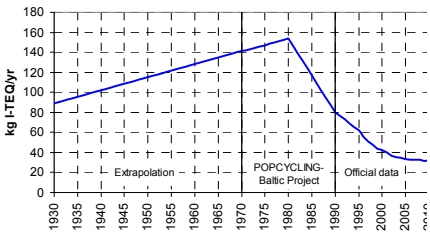

Fig. 1.8. *Emission to soil in the EMEP region used in scenario calculations.*

Spatial distribution of emissions

For the construction of spatial distribution of emissions to soil for each year from the considered period for all emission sectors except for industry and agricultural activities population density was used as surrogate. The emissions from agricultural activities were spatially distributed in accordance with fractions of arable land area in the corresponding grid cells. For industrial emissions it was supposed that spatial distribution of emissions to land is proportional to that to the atmosphere taken from TNO emission estimates for 2000. The latter supposition is based on the fact that correlation between emissions to soil in 1994 taken from the above EU project and TNO estimates of emissions to air is rather high (0.7).

Spatial distribution of emissions to soil for 1994 calculated by the above-described procedure is shown in Fig. 1.9.

Unfortunately, no information on emissions to soil outside the EMEP region is available, so that emissions from the USA, Canada, Japan and other regions within the Northern Hemisphere were not taken into account. Certainly, this can lead to certain underestimation of PCDD/F pollution levels in the EMEP domain due to underestimation of the intercontinental transport of the pollutant previously accumulated in soils outside the EMEP region due to emissions to soil.

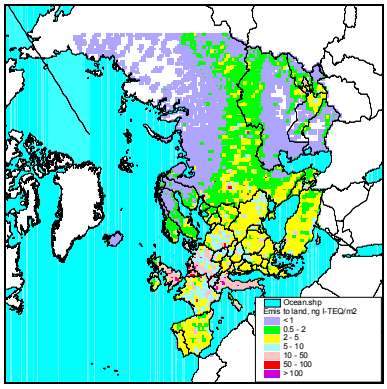

Fig. 2.9. *Spatial distribution of emission to soil in the EMEP region for 1994 used in scenario calculations.*

1.2.2. Calculation results

With the above constructed scenario calculations of PCDD/F contamination taking into account PCDD/F emissions both to soil and the atmosphere were performed from 1930 to 2010 by hemispheric version of MSCE-POP model. The comparison of calculated values of PCDD/F total toxicity with available measurements is shown by scatter plot in Fig. 1.10. As above, measurements in contaminated regions and outliers are not taken into account in the comparison.

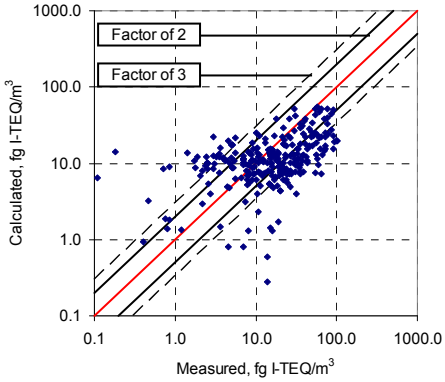

Fig. 1.10. *The comparison of PCDD/F air concentrations measured within the period from 1990 to 2010 with calculations taking into account emissions both to air and to soil.*

The correlation between measurements and calculations amounts to 0.56, and relative bias is about – 40%. Further, over 70% of calculated values agree with measurements within a factor of three, and among them about 45% agree within a factor of two. The comparison shows that the results of simulations using the above scenario still underestimate measured values, however, the agreement of measurements with calculations made on the basis of the constructed scenario is much better than with calculations taking into account emissions to the atmosphere only (cf. Fig. 1.5 above).

The discrepancies between calculations and measurements can be partly explained by inhomogeneity of measurement data obtained at location of different types (from industrial to background) and, possibly, with the use of different analysis techniques. So, to obtain more robust comparison, it is reasonable to compare measurements and calculations averaged at annual levels. Such comparison is shown in Fig. 1.11, where ranges of measured values within a year are also shown.

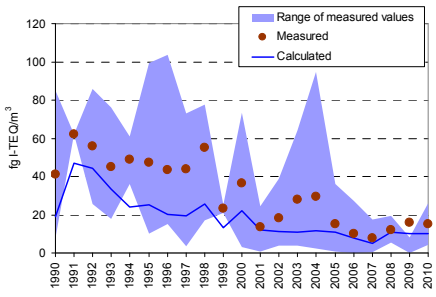

Fig. 1.11. *The comparison of PCDD/F air concentrations measured within the period from 1990 to 2010 with calculations taking into account emissions both to air and to soil, annual averages.*

The comparison of measured and calculated values of PCDD/F total toxicity on the level of annual averages shows that calculated values in most cases are within the range of measurements. The correlation between measurements and calculation results is 0.89 and about 70% of calculated annual averages agree with measurements within a factor of 2. However, the comparison on the level of annual averages

confirms that calculations underestimate PCDD/F total toxicity 1.7 times on the average. The reasons of the obtained underestimation are as follows:

1. Usage of measurements made at locations of different type by different equipment. From this viewpoint, collection and evaluation of national PCDD/F measurement data could be of use for further refinement of model evaluation of the environmental pollution by PCDD/Fs.

2. Rough representation of temporal trend of emissions to soil. It was supposed that the trends of emissions to soil and to the atmosphere are similar. However, it is clear that emission reductions of emissions from different emission sectors are different. However, according to available emission data sectoral composition of emissions to soil and to the atmosphere is different (Fig. 1.12). Expert estimates of historical data for emissions to soil could help the refinement of model evaluation of PCDD/F environmental contamination.

3. Inclusion of emissions to soil outside the EMEP domain (USA, Canada, China, Japan, etc.) can refine the agreement between measurements and calculation results.

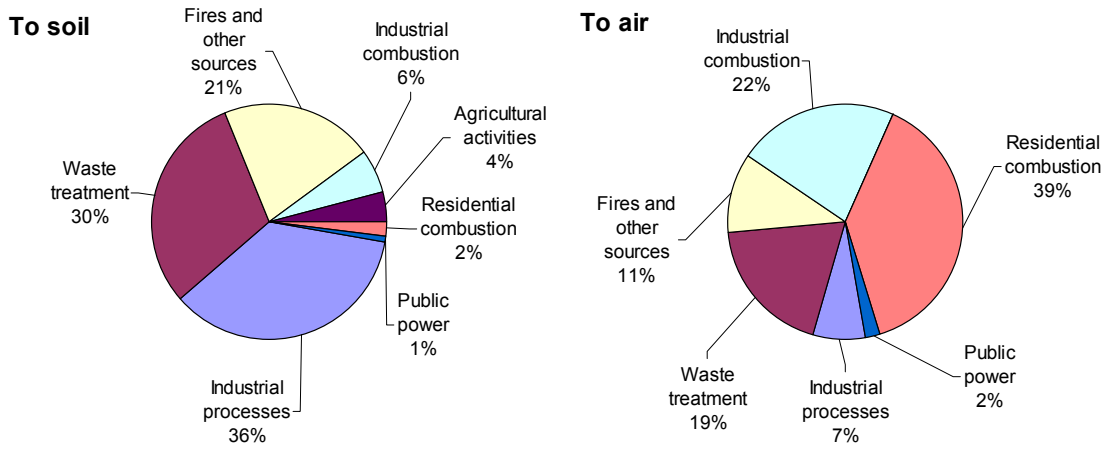

Fig. 1.12. *Comparison of sectorial conposition of emissions to soil and to the atmosphere.*

1.3. Global-scale modelling of POP pollution

Last years MSC-East pays great attention to the development of global-scale modelling of persistent organic pollutants. Special POP modules for the GLEMOS model are developed; test simulations of POP transport in the environment are carried out. This year the module describing POP behaviour in vegetation was implemented in GLEMOS. Long-term calculations of the dispersion and accumulation in the environmental media of two POPs with significant potential to the long-range transport (HCB and PCB-153) were made. Some of the obtained results are presented in this section.

1.3.1. Evaluation POP modules for the GLEMOS model

The GLEMOS (Global EMEP Multi-media Modelling System) has modular structure [*Travnikov et al.*, 2009]. Specific modules describing different environmental media and different pollutants can be attached to or detached from the model at the compilation stage depending on the task. Previous test global-scale model runs for POPs were conducted with the consideration of three media: the

atmosphere, the ocean, and soil [*Jonson and Travnikov*, 2012]. Last year the fourth medium was added: vegetation module was attached to GLEMOS. This module describes the accumulation of POPs both in vegetation itself and in forest litter as well as gaseous exchange between the atmosphere and vegetation and pollutant flux with defoliation. POP fluxes from the atmosphere to vegetation (dry and wet deposition) and from forest litter to soil (decomposition) are modelled in the separate exchange GLEMOS module. Current model configuration related to POPs modelling is presented in Fig. 1.13.

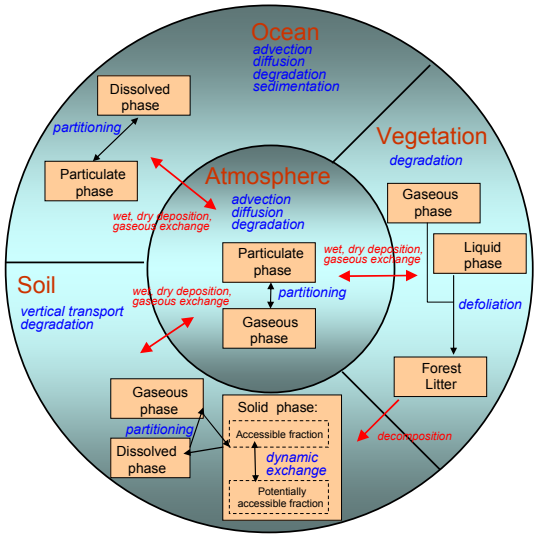

Fig. 1.13. *The scheme of the main processes related to POPs in the current version of the GLEMOS model*

1.3.2. Modelling PCB-153 global transport

The simulations of PCB-153 transport in the environment were conducted to test new configuration of the GLEMOS model, to investigate the processes of pollutant accumulation in media, to estimate the influence of input meteorological data to model output data. Three global-scale model runs were done.

1. Long-term run (1930-2011) on 3^0x3^0 model grid

2. Short-term run (2009-2011) on 1^0x1^0 grid with input meteorological data prepared by the WRF model [*Michalakes et al.,* 2004; *Skamarock et al.,* 2005]

3. Short-term run (2009) on 1^0x1^0 grid with GEM input meteorological data, prepared by the GEM model [*Côté et. al*., 1998a; *Côté et. al.,* 1998b; *Yeh et. al.,* 2002]

Below the description of modelling results is presented.

Simulation of long-term accumulation in media on 3^0x3^0 grid. Calculations for 82-year period of time (1930-2011) on 3^0x3^0 global grid have been performed. The main purposes of these computations were investigation of the processes of PCB-153 accumulation and degradation in media and the preparation of the initial data for short-term modeling with higher spatial resolution.

Gridded historical anthropogenic emission data were compiled on the basis of “maximum” and “default” scenarios of the global inventory [*Breivik et al.,* 2007] (Fig. 1.14). It can be seen that emission curve has maximum in 1975 (29 t/y). In recent years total anthropogenic emissions decrease monotonously.

Calculated time trends of PCB-153 content in environmental media follow the shape of emission time trend with some delay (Fig. 1.15). Maximum delay (13 years) takes place for soil medium, minimum (1 year) – for air.

Most of PCB-153 mass is accumulated in soil: from 53% in 1930 to 80% in 2011 (Fig. 1.16). The shares of seawater and vegetation in PCB-153 mass balance vary from several percent to several tens percent. The atmosphere contains <1% since 1978.

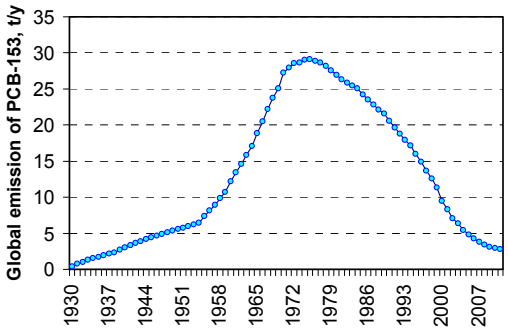

Fig. 1.14. *Time trend of PCB-153 global anthropogenic emissions (1930-2010)*

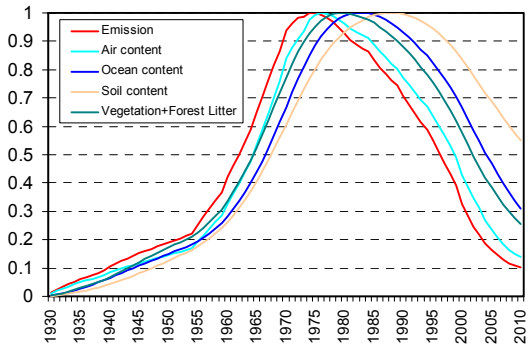

Fig. 1.15. *Time trends of PCB-153 content in environmental media*

Recent years the most part of PCB-153 mass is removed from the environment due to soil degradation (Fig. 1.17). This process is responsible for ~51% of total removal in 2011. The contributions of removal from the ocean (degradation and sedimentation) amount to ~29% in 2011, degradation in vegetation - 14%. The relative importance of the removal from air decreases from year to year (from 62% in 1930 to 6% in 2011).

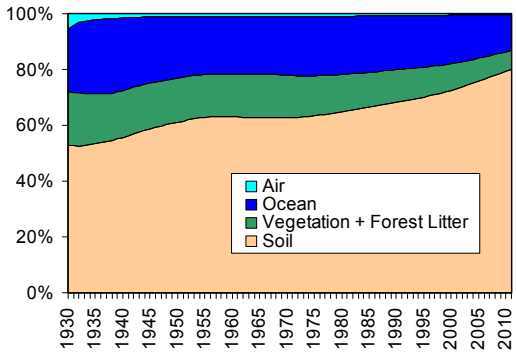

Fig.1.16. *The percentage of PCB-153 content in environmental media for time period from 1930 to 2011*

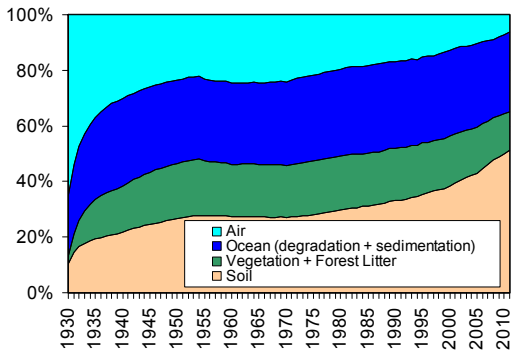

Fig. 1.17. *The percentage ratio of different ways of PCB-153 removal from environmental media for time period from 1930 to 2011*

Relative contributions of historical re-emissions of PCB-153 from media and anthropogenic air emissions in 2011 were evaluated. Fig. 1.18 shows that these contributions are comparable. The field of air concentration conditioned by historical emission is smoother. Emissions from media make a greater contribution in remote regions, anthropogenic emissions of 2011 are the most important in polluted regions.

The EMEP region as the source and the receptor of PCB-153 mass in the atmosphere was considered separately. According to calculations results, internal sources of anthropogenic emissions and re-emissions make the largest contribution to the pollution of the EMEP region (Fig. 1.19). EMEP sources give ~91% of PCB-153 mass in the atmosphere within the EMEP boundaries (Fig. 1.19) but only ~32% of total PCB-153 content in the atmosphere (Fig. 1.20). The shares of anthropogenic emissions and historical re-emissions are comparable both inside and outside the EMEP region both for EMEP and non-EMEP sources.

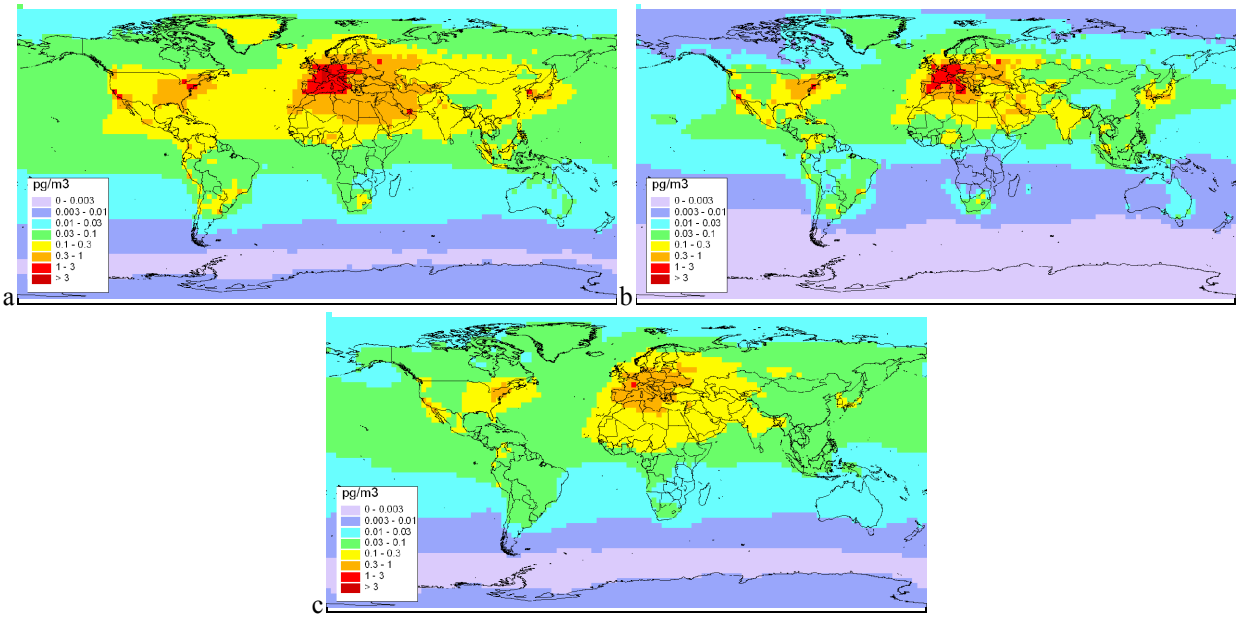

Fig. 1.18. *Spatial distributions of PCB-153 annual mean concentration in air for different emission scenario:*
a – anthropogenic emissions of 2011 + historical emissions;
b - anthropogenic emissions of 2011 only;
c - historical emissions only

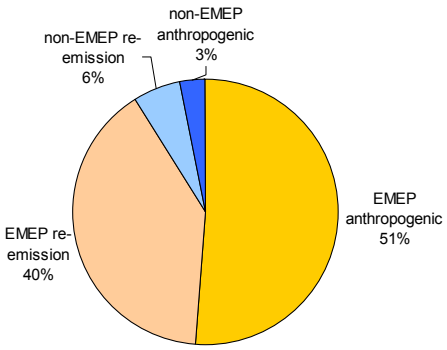

Fig. 1.19. *Relative contributions of different emission sources to PCB-153 air content inside the EMEP region*

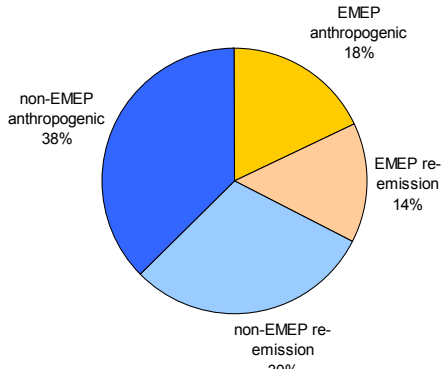

Fig. 1.20. *Relative contributions of different emission sources to PCB-153 in the atmosphere over the entire globe*

Short-term simulation on 1^0x1^0 grid. The results of 82-year spin-up from 1930 on 3^0x3^0 grid has been employed as initial conditions for 1^0x1^0 model runs. Two simulations with different input meteorological data were conducted: three-year run (2009 – 2011) with WRF meteorology and annual run (2009) with GEM data.

Fig. 1.21 shows modelled spatial distributions of PCB-153 annual mean air concentrations in 2009 obtained using different input meteorological data. It can be seen, that concentrations fields are similar over polluted regions as well as over remote regions.

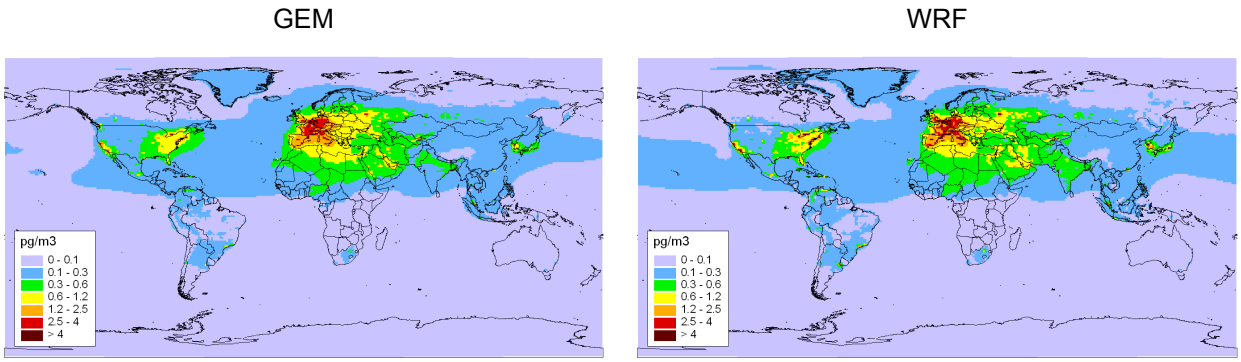

Fig. 1.21. *Spatial distributions of PCB-153 annual mean concentration in air calculated with GEM (left) and WRF (right) input meteorological data.*

The spatial distributions of PCB-153 annual mean concentrations media other than atmosphere for 2011 are given in Fig. 1.22.

Elevated level of pollution in soil is characteristic of Europe and North America (Fig. 1.22a). In the most polluted central part of Europe soil concentrations exceed 30 pg/g. The range 10-30 pg/g can be assumed as background for Europe, 2-10 pg/g – for North America.

The highest concentrations of PCB-153 in seawater (> 0.15 pg/l) take place near European coast (Mediterranean Sea, North Sea, etc.). The levels of 0.03-0.15 pg/l are typical for the middle latitudes of the Northern Hemisphere. Concentrations in the Southern Hemisphere are less than 0.01 pg/l.

Maximum levels of PCB-153 concentrations in vegetation (> 1000 pg/g) occur in the Northern Hemisphere too, but the spatial distribution of concentration differs from the spatial distribution of emission substantially. The character of the distribution of PCB-153 content in vegetation is largely determined by the vegetation properties and the peculiarities of interaction between different forms of PCB-153 in air, vegetation, and soil.

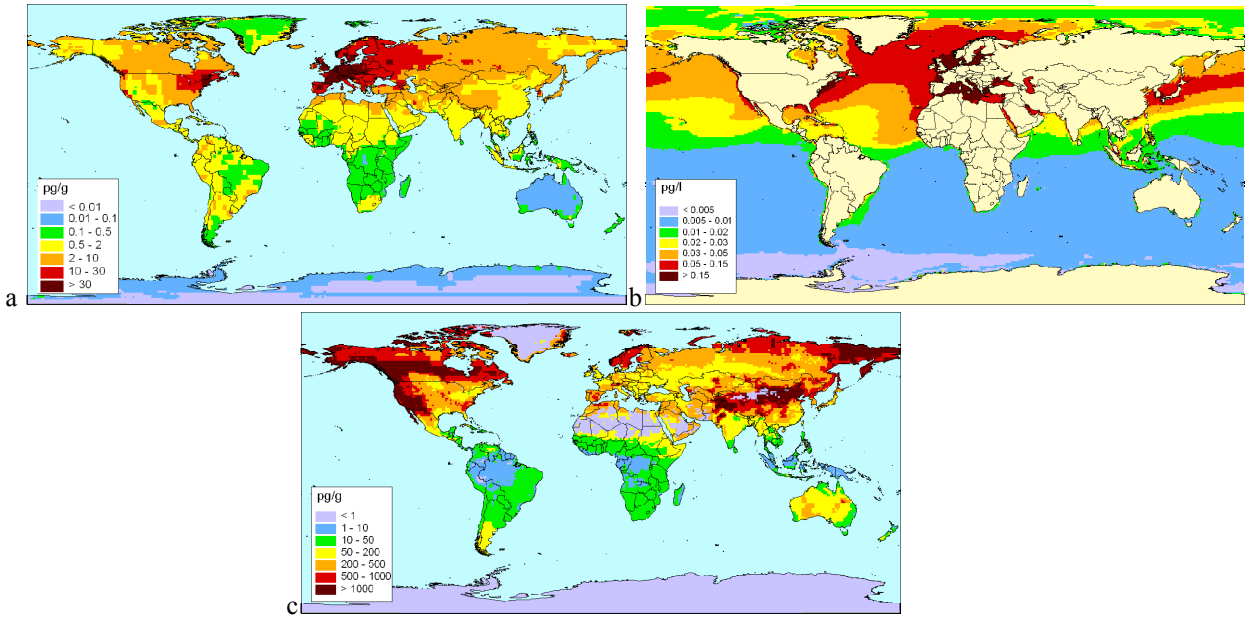

Fig. 1.22. *Spatial distributions of PCB-153 annual mean concentrations in soil(a – top 5-cm), seawater (b – upper layer), and vegetation (c) in 2011*

Comparison with measurements. The results of modelling on 1^0x1^0 grid for 2009-2011 have been compared to measurement data on PCB-153 concentrations in air obtained at the EMEP monitoring network. Annual and monthly mean concentrations were considered. Some results are presented in Fig. 1.23, 1.24.

The model slightly underestimates contamination levels of PCB-153 in the EMEP region (Fig. 1.23). Annual mean modeled values are below measured ones at most sites. There is high spatial correlation of annual mean modeled and measured concentrations in air. The correlation coefficients equal 0.83, 0.95 and 0.87 in 2009, 2010 and 2011, respectively.

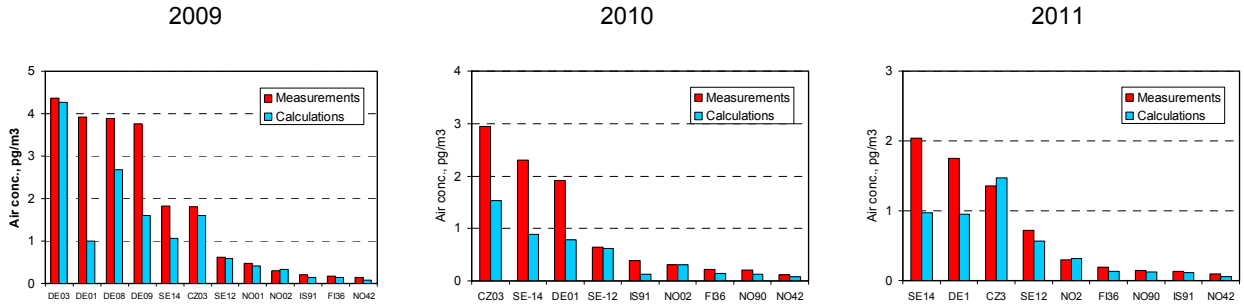

Fig. 1.23. *Annual mean PCB-153 concentrations in air calculated by the GLEMOS model and measured at the EMEP monitoring sites in 2009-2011*

Table 1.2 contains statistical indicators describing the agreement between calculated and measured annual mean air concentrations at the EMEP sites in 2009. Information for model runs with variable input meteorological data and variable grid resolutions is presented. It can be seen that the increase of spatial resolution improves the agreement between modeled and measured data. At the same time, the change of input meteorology (from GEM to WRF data) does not substantially affect basic statistical indicators.

Table.1.2. *Statistical indicators for different model runs*

№	Grid resolution	Input meteorology	BIAS, pg/m^3	Correlation coefficient
1	30x30	GEM	-0.76	0.71
2	10x10	GEM	-0.60	0.81
3	10x10	WRF	-0.62	0.83

The temporal changes of monthly mean air concentrations of PCB-153 are in accordance with measurements for most of the EMEP sites. Fig. 1.24 presents examples for two stations: Swedish site SE12 and Finnish site CZ03. It can be seen that the model has reproduced most of the peculiarities of measured time trends.

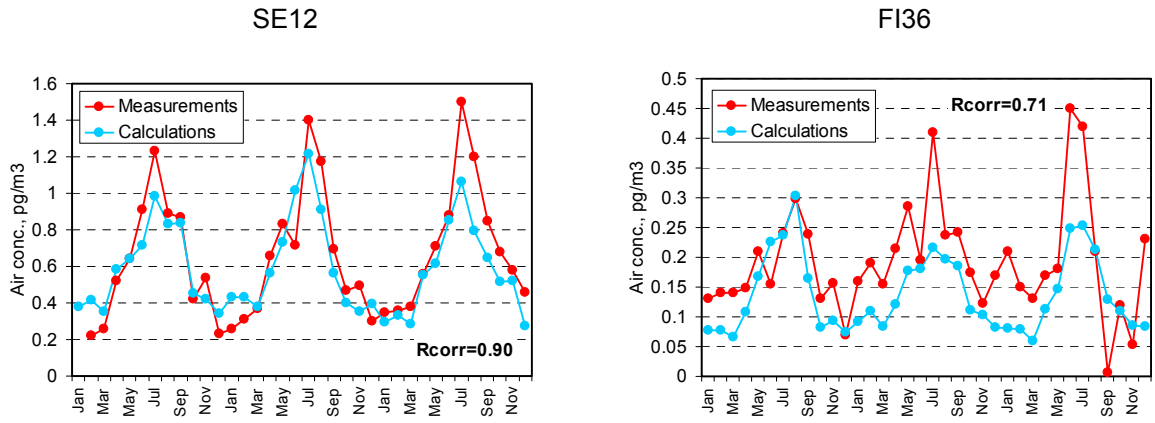

Fig. 1.24. *Monthly mean PCB-153 concentrations in air calculated by the GLEMOS model and measured at the EMEP monitoring sites SE12 and FI36 in 2009-2011*

The results of 3^0x3^0 calculations of PCB-153 concentrations in upper soil level have been compared with surface soil measurements of PCB-153/132 performed at 191 background sites worldwide in 1998 [*Meijer et al.,* 2003]. To reduce significant dispersion of observational data (spread in measured values exceeds an order of magnitude in some 3^0x3^0 model grid cells), they were grouped and replaced by arithmetic means in grid cells. The resulting scatter plot of observed and calculated soil concentrations is given in Fig. 1.25. In general, measured values exceed calculated ones substantially. High vertical gradient of PCB-153 soil concentration near ground surface seems the main reason for this: maximum levels of concentration can not be reproduced by the model due to limited vertical spatial resolution of the model grid. At the same time, there is noticeable correlation between measured and modelled values in logarithmic scale. Taking into account significant scatter of the observed soil concentrations, the results of the comparison can be considered as reasonable.

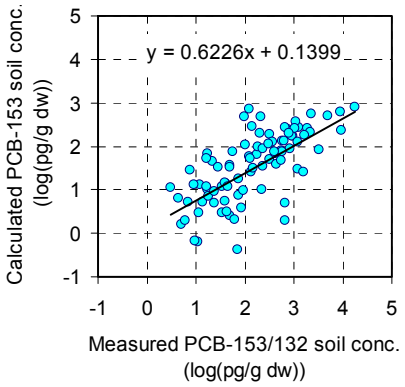

Fig. 1.25. *Scatter plot of calculated soil concentrations of PCB-153 in the highest soil level and measured soil concentrations of PCB-153/132 (dw – dry weight of soil)*

1.3.3. Modelling HCB global transport.

For the investigation of HCB transport and accumulation in the environment two global-scale runs of the GLEMOS model have been done:

1. Long-term run (1930-2011) on 3^0x3^0 grid with GEM input meteorological data;
2. Short-term run (2011) on 1^0x1^0 grid with WRF input meteorological data.

Below the description of modelling results is presented.

Simulation of long-term accumulation in media on 3^0x3^0 grid. A scenario of historical HCB emissions was constructed for modelling of long-term accumulation of the pollutant in the underlying surface.

According to this scenario, global HCB emissions were increasing during the period from 1945 to 1978 reaching 18 thousand tonnes in the end of the period (Fig. 1.26). Further (in 80th of the previous century) emissions have been reduced rapidly with subsequent moderate decrease (about 10% a year on the average) beginning from 1987. Total emissions of HCB in 2011 amounted to 45 tonnes.

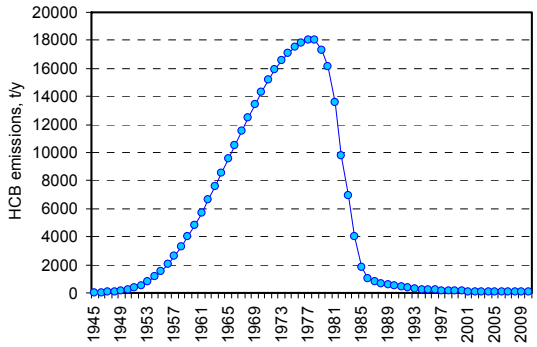

Fig. 1.26. *Time trend of HCB global anthropogenic emissions (1945-2010)*

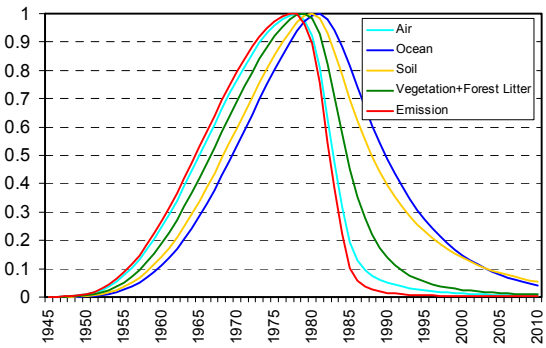

Fig. 1.27. *Time trends of HCB content in environmental media*

The behaviour of HCB in the environment differs from that of PCB-153 described above due to differences in physical - chemical properties of two mentioned pollutants in media and to differences in anthropogenic emissions profiles. For HCB the most inertial media is ocean. The peak of time trend of HCB content in the ocean has maximum (3 - year) delay relative to emission peak (Fig. 1.27). Air content curve peak has not such delay - air is the least inertial medium. Soil and vegetation have intermediate positions between ocean and air. Time delays of HCB environmental content curves relative to emission curve (Fig. 1.27) are less than those for PCB-153 (Fig. 1.15), because HCB is characterized by higher degradation constants in all the media.

According to simulation results, the ocean contains 55-70% of total environmental content of HCB. Relative soil content is about 30% – 40%. Soil is not able to accumulate such a high fraction of HCB as for PCB-153. The share of HCB in the atmosphere is continuously decreasing from ~30% in the end of 40th previous century to ~ 1% in XXI century (Fig. 1.28).

The most part of HCB mass is removed from the environment due to ocean degradation and sedimentation (Fig. 1.29). These processes are responsible for ~70-80% of total removal in the last years. The contributions of soil degradation amount to ~15-20%. The relative importance of the removal from air decreases from 59% in 1945 to 3% in 2011.

Vegetation (with forest litter) is the least important medium in HCB mass balance. It contains much less than 1% of HCB in the environment in the last years, the role of vegetation in removal processes is negligible too. From the other hand, vegetation occurs to be a kind of “transport media” from the atmosphere to soil.

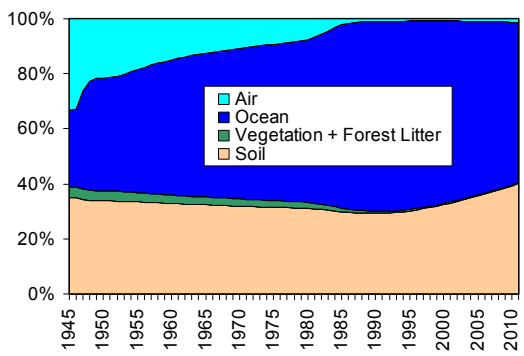

Fig. 1.28. *Fractions of HCB content in environmental media for time period from 1945 to 2011*

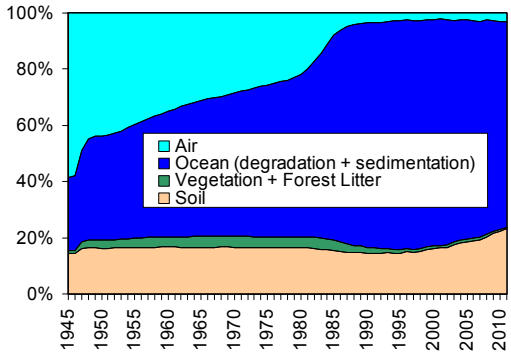

Fig. 1.29. *Relative contributions of different ways of HCB removal from environmental media for time period from 1930 to 2011*

Historical re-emissions of HCB play an extremely important role in the formation of spatial distribution and levels of air pollution all over the world except of south-east Asia, where the contribution of anthropogenic sources of 2010 is important (Fig. 1.30). This can be explained mainly by sharp drop of HCB anthropogenic emissions (especially in 1980-s); emission reduction from 1978 (year of maximum) to 2011 is ~390 times. For comparison, the corresponding decrease in anthropogenic emissions of PCB-153 from 1975 to 2011 is ~10 times.

Reduction of emission in south-east Asia was not as considerable as in other regions. Therefore anthropogenic emissions make the largest contribution to air content of HCB there.

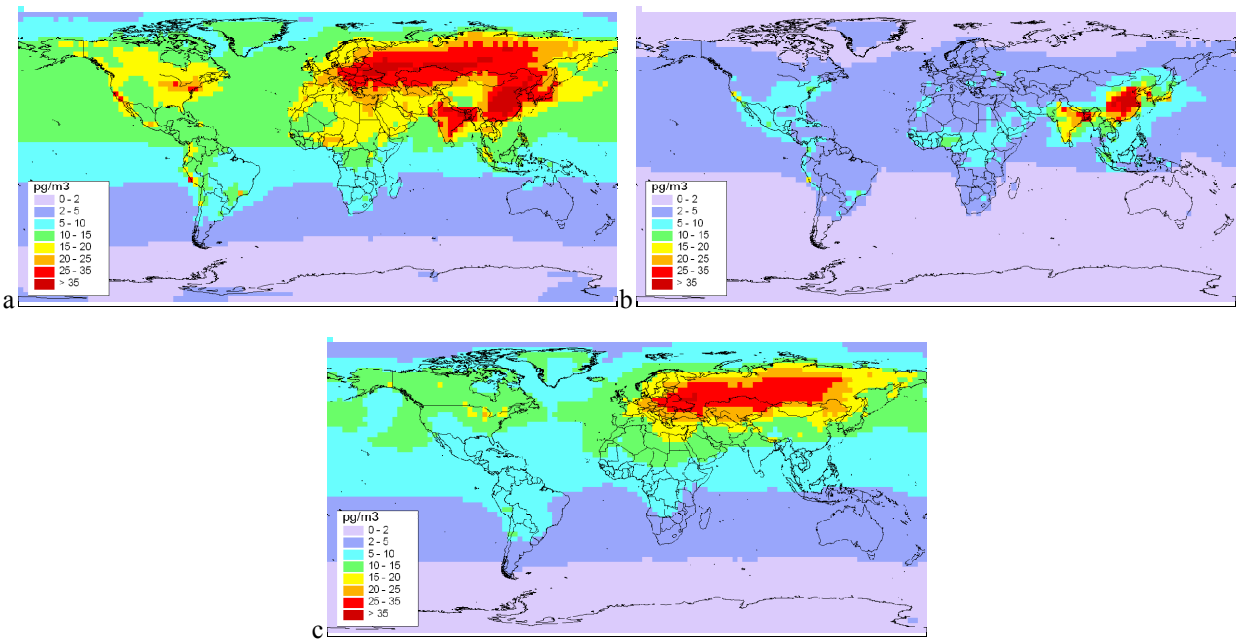

Fig. 1.30. *Spatial distributions of HCB annual mean concentration in air for different emission scenario:*
a – anthropogenic emissions of 2010 + historical emissions;
b - anthropogenic emissions of 2010 only;
c - historical emissions only

According to the modelling results pollution of the EMEP region by HCB is dominated by the secondary emission sources, while contribution of anthropogenic emissions is comparatively small. The intercontinental transport of HCB significantly influences the pollution levels in the EMEP region. Particularly, the share of non-EMEP emission sources accounts for 35% (Fig. 1.31) from which 24% is contributed by the non-EMEP secondary emissions and 11% by the non-EMEP anthropogenic emissions.

Outside the EMEP region the contribution of anthropogenic emissions sources to HCB air content is comparable to that of re-emissions (Fig. 1.32). Non-EMEP sources play the most important role in the global HCB air pollution in 2010 (76% of total air content).

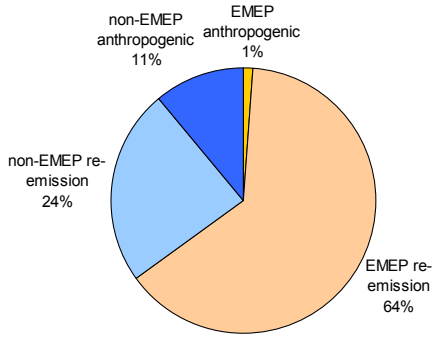

Fig. 1.31. *Relative contributions of different emission sources to HCB air content inside the EMEP region*

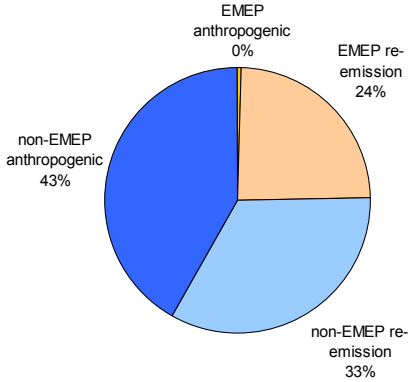

Fig. 1.32. *Relative contributions of different emission sources to HCB mass in the atmosphere over the entire globe*

Short-term simulation on 1^0x1^0 grid. One annual global-scale GLEMOS model run on 1^0x1^0 grid was done. The modelling of HCB transport in the environment in 2011 was conducted with the initial conditions prepared on the base of the results of 67-year 3^0x3^0 spin-up described above. Input meteorological data were prepared with the help of WRF model. The same emission scenario as for 3^0x3^0 was used. Fig. 1.33 presents calculated spatial distributions of annual mean HCB concentrations in media.

Maximum HCB concentrations (> 45 pg/m^3) in the atmosphere have been found in Europe, the Russian Federation, India and China. Outside highly contaminated regions air concentrations are close to background ones that depend on latitude. In particular, background HCB air concentrations in low and temperate latitudes of the Northern Hemisphere amount to 15-20 pg/m^3 (Fig. 1.33[a]).

Spatial pattern of HCB soil concentrations reflects the peculiarities of historical accumulation of the pollutant. Maximum contamination in soil takes place in areas with high emissions and in regions with high latitudes due to cold condensation process. Highest soil concentrations are characteristic of Europe and Russia where they exceed 100 pg/g (see Fig. 1.33[b]).

The distribution of HCB concentrations in surface seawater layer is given in Fig. 1.33. There is evident latitudinal dependence of pollution level. The highest values of HCB concentrations in seawater (more than 3 pg/L) were obtained for high-latitude regions of the Northern Hemisphere. The reason for this is strong temperature dependence of the gaseous flux from air to water: lower air temperatures correspond to higher air-water flux. Seawater HCB concentrations in the Antarctic region are higher than those in the temperate latitudes of the Southern Hemisphere.

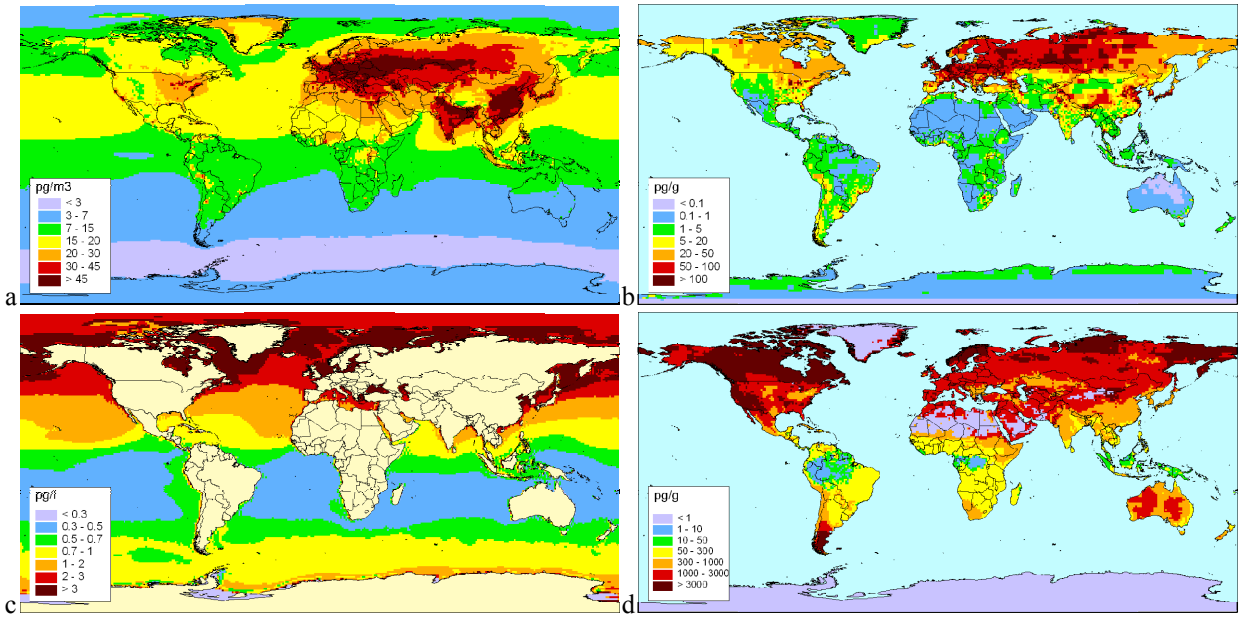

Fig. 1.33. *Spatial distributions of HCB annual mean concentration in air (a), soil (b), seawater (c), and vegetation (d) for 2011*

Spatial distribution of HCB content in vegetation (Fig. 1.33[d]) differs from that in atmosphere and soil. As already mentioned when describing PCB-153 pollution, it is influenced by the properties of vegetation and the peculiarities of pollutant mass exchange between media. Maximum HCB content in vegetation (> 3000 pg/g) takes place in northern regions of Europe and Russia and in Canada.

Comparison with measurements. Annual mean HCB air concentrations calculated by the GLEMOS model on $3^{0x}3^{0}$ global grid for the last two decades were compared to the results of measurements at North American monitoring sites (data of Stockholm Convection on POPs) and EMEP sites (Fig. 1.34, 1.35). Most of the measured values are inside the ranges of calculated values for North America and the EMEP region. At the same time, calculated trend of air concentrations is more drastic than the measured one. Possible reasons for this could be the underestimation of anthropogenic emissions in recent years and/or defects of parameterization of exchange processes between environmental media.

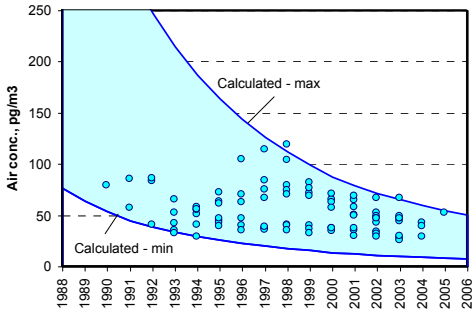

Fig. 1.34. *Annual mean air concentrations of HCB measured at North American sites (blue points) and calculated by the GLEMOS model (range of concentrations over North America)*

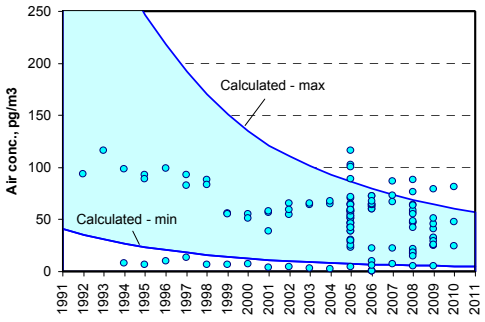

Fig. 1.35. *Annual mean air concentrations of HCB measured at EMEP sites(blue points) and calculated by the GLEMOS model (range of concentrations over EMEP region)*

Annual mean HCB concentrations in air in 2011 calculated on $1^{0x}1^{0}$ grid were compared to measurement data of EMEP monitoring network. The results are presented in Fig. 1.36.

At most stations measured values exceed calculated ones within a factor of 2. Greatest difference between measurements and calculations take place at Norwegian site NO42. The possible reason of such disagreement - local emission sources near Spitsbergen – is discussed in [*Shatalov et. al.*, 2012].

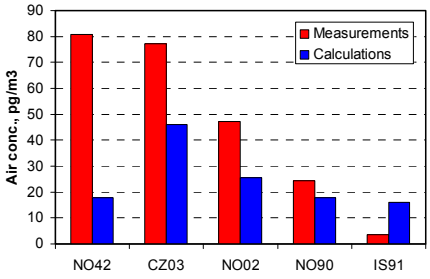

Fig. 1.36. *Annual mean HCB concentrations in air calculated by the GLEMOS model and measured at the EMEP monitoring sites in 2011*

1.4. Concluding remarks

The main outcome of the work on further refining POP modelling tools can be formulated as follows.

Possible directions of refinement of model description of POP gas-particle partitioning and degradation in particle-bound form were investigated for B[a]P as typical representation of POPs with essential part of particulate form. It was found that:

- In spite of small fraction of EC in the atmospheric aerosol the share of B[a]P sorbed on EC is essential due to high sorption capacity of this aerrosol compound.
- Degradation rates of B[a]P sorbed on aerosol compounds of different chemical nature are essentially different. In particular, stability of B[a]P sorbed on EC in the atmosphere is much higher than that sorbed on aeerosols of other chemical natuer (OC or mineral compounds).
- Further work on the modification of model description of gas-particle partitioning and degradation of particle-bound POPs can result in further refinement of the agreement between measurement data and model predictions.

The influence of direct emissions of POPs to the environmental media other than the atmosphere was evaluated for PCDD/Fs with the use of data of national measurement campaigns collected by MSC-E from the literature. The results of this evaluation are:

- Underestimation of PCDD/F levels can be partly explained by omitting emissions to media other than the atmosphere.
- Collection and evaluation of national PCDD/F measurement data under EMEP could be of use for further refinement of model evaluation of the environmental pollution by PCDD/Fs.
- Expert estimates of long-term trends of PCDD/F emissions to soil can lead to more reliable evaluation of environmental pollution of the EMEP region by PCDD/Fs.
- Information on emissions of PCDD/F to soil for non-EMEP regions is desirable.

The work on the development of POP modules for the GLEMOS model and on the global-scale modeling of the transport of POPs was continued. The following main results have been obtained.

- The module describing the behavior of POPs in vegetation and forest litter was added to the GLEMOS model.

- The series of long-term and short-term simulations of HCB and PCB-153 transport and accumulation in the environment was carried out using the last version of the GLEMOS models. Calculations showed the following.

  Most part of PCB-153 mass in the environment (more than 60%) is contained in soil. Soil degradation is responsible for ~ 50% of total removal of PCB-153 in recent years. The least capacious and inertial media is air: it is responsible for <1% total content in the environment and 10-20% of degradation. Relative contributions of historical re-emissions and anthropogenic emissions to air pollution by PCB-153 are comparable last years.

  According to simulation results, the ocean contains 55-70% of total environmental content of HCB. Soil content is about 30% – 40%. The most part of HCB mass is removed from the environment due to ocean degradation and sedimentation. These processes are responsible for ~70-80% of total removal in the last years. Vegetation is the least important medium in HCB mass balance. It contains much less than 1% of HCB in the environment in the last years, the role of vegetation in removal processes is negligible too. Historical re-emissions of HCB play extremely important role in the formation of spatial distribution and levels of air pollution all over the world except of south-east Asia, where the contribution of anthropogenic sources is important last years.

  The results of model calculations are in satisfactory accordance with the available measurement data.

Further work on the development of the capabilities for global-scale modelling of POP transport could be carried out in the following directions:

- Development of ice/snow module for the GLEMOS model.
- Refinement of parameterizations of POP processes in the environmental media.